Hindawi
Advances in Polymer Technology
Volume 2019, Article ID 2318347, 11 pages
https://doi.org/10.1155/2019/2318347

Research Article

Enhancing Mechanical and Thermal Properties of Polyurethane Rubber Reinforced with Polyethylene Glycol-g-Graphene Oxide

Li Wang[1], **Wen Fu**[2], **Wenlong Peng**[2], **Haotuo Xiao**[2], **Shenglin Li**[2], **Jianning Huang**[2] **and Cuiwen Liu**[2]

[1]*College of Chemical Engineering, Guangdong University of Petrochemical Technology, Maoming 525000 Guangdong, China*
[2]*College of Material Science, Guangdong University of Petrochemical Technology, Maoming 525000 Guangdong, China*

Correspondence should be addressed to Wen Fu; a449192213@163.com

Received 5 June 2019; Accepted 21 July 2019; Published 5 August 2019

Guest Editor: Hong Liang

This paper attempted to achieve the purpose of increasing the tensile strength and toughness of polyurethane rubber (PUR) simultaneously by introducing polyethylene glycol (PEG) onto the surface of graphene oxide (GO) to introduce hydrogen bond interactions into the PUR-GO system. GO was grafted with PEG and added to PUR by mechanical blending. The polyethylene glycol-g-graphene oxide (MGO) was characterized by infrared spectroscopy, Raman spectroscopy, X-ray diffraction, and thermogravimetric analysis. The PUR/MGO composites were tested by tensile testing machine, thermogravimetric analysis, dynamic thermal analysis, and scanning electron microscopy. The results demonstrated that PEG was successfully grafted onto the surface of GO and the grafting rate was about 37%. The grated PEG did not affect the crystalline structure of GO. The addition of MGO could improve the thermal stability of PUR vulcanizate. After the addition of GO, the glass transition temperature (T_g) of vulcanizate was shifted to higher temperature. However, the T_g of vulcanizate reinforced by MGO was shifted to lower temperature. The strength and toughness of vulcanizate were significantly improved by adding MGO. The reason was that the hydrogen bond interactions between MGO and PUR were destroyed and the hidden length was released during the strain process. A lot of energy was consumed, and thus the strength and toughness of PUR vulcanizate were improved.

1. Introduction

Generally, raw rubber without reinforcer has poor mechanical properties. For most practical applications, the rubber should be reinforced with some additives. Carbon black and silica are the commonly used reinforcing agents. In recent years, graphene has been studied as a new type of reinforcing agent for rubber. The Young's modulus of monolayer graphene is about 1.1 TPa and the fracture strength is 125 GPa [1]. Hence, graphene should have promising prospect in the field of rubber reinforcement [2–4]. However, it was reported that graphene could increase the strength of rubber matrix but will damnify the toughness and ductility [5–7]. How to optimize the strength and toughness of graphene reinforced rubber is still an important issue in the field of material science.

Natural biomaterials such as spider silk and animal bone always exhibit an amazing balance among the strength, toughness, and ductility. Studies have revealed that it is due to the sacrificial bonds and hidden length at the soft-hard interface, so these natural biomaterials can achieve both high strength and ductility [8–10]. Inspired by the structure of these natural biomaterials, some reports about constructing sacrificial bonds at the interface between inorganic filler and elastomer to increase the strength and toughness of materials have emerged recently. The strength of noncovalent sacrificial bonds, such as hydrogen bond [11, 12], π-π conjugate interactions [13], π-cation interactions [14], and ionic bonds [15], are weak, however, through the breaking of reasonable sacrificial bonds and sliding of some chain segments the interfacial load could be transferred and the strength could be enhanced.

Tang [16] constructed a network of sacrificial metal-ligand bonds in pyridyl styrene-butadiene rubber (VPR) and achieved 27.8 MPa tensile strength of the vulcanizate, which was higher than that of VPR reinforced by carbon black and silica. Huang [17] modified solution polymerized

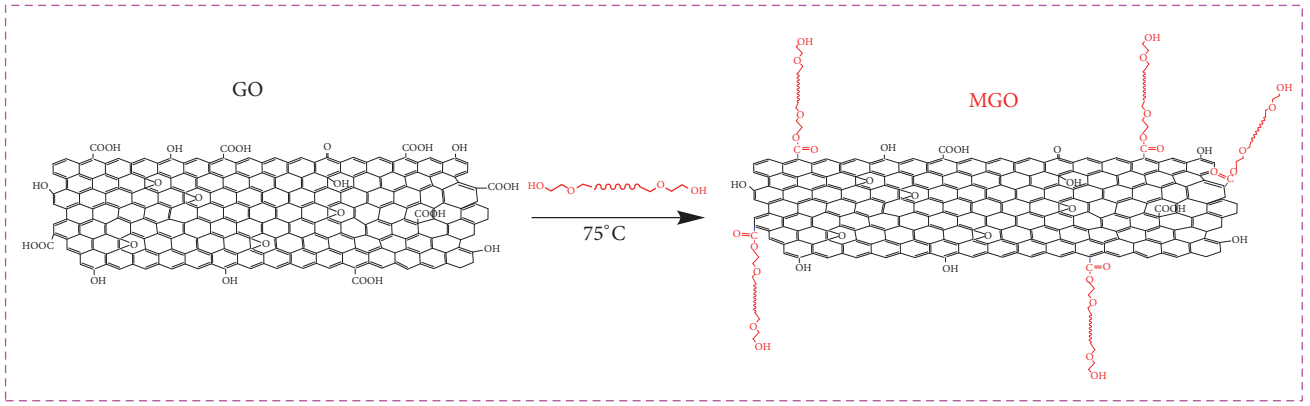

Figure 1: Preparation of polyethylene glycol graft modified graphene oxide.

styrene butadiene rubber (SSBR) with triazolidinedione by click chemistry and introduced the urezo groups to SSBR to provide hydrogen bonds; thereby, the sacrificial bonds were constructed in the system. The tensile strength of the modified SSBR had been significantly enhanced to 7.64 MPa, which was higher than that of the pure SSBR. Wu [18] used the maleic anhydride-modified polyisoprene rubber and aminomodified carbon nanodots to construct the network of sacrificial bonds and used unsaturated bonds to construct the chemically cross-linked network. The tensile strength approached 30.5 MPa when the dosage of carbon nanodots was only 3 phr, which was stronger than that of the polyisoprene rubber reinforced by 40 phr N330 carbon black. Mao [19] added a kind of VPR into GO/styrene butadiene rubber (SBR) system and constructed ionic bond interaction between pyridine group (positive) in the vinyl pyridine unit of VPR and oxygen-containing functional group (negative) on the surface of GO. Wu [20] characterized the interfacial interaction of VPR/GO composites by the dielectric relaxation spectra of the vulcanizates with different interactions (ionic bond, hydrogen bond). The results revealed that the velocity of segmental relaxation and interfacial relaxation of VPR/GO composite bonded by ionic bond was higher than that of composites bonded by hydrogen bond, indicating that the internal interaction of GO/VPR composites bonded by ionic bond was stronger. Li [21] found that the dissociation energy of hydrogen bond in polyurethane was about 16.7 kJ/mol. In general, the bonding energy of C-C covalent is over 300 kJ/mol. It means that the hydrogen bond is likely to be destroyed during the strain process and additional strain energy will be consumed, so the strength and toughness of material are guaranteed.

In the present paper, graphene oxide was grafted with polyethylene glycol 600 by means of the reaction between the carboxyl groups on the surface of graphene oxide and the hydroxyl groups at the end of polyethylene glycol and then added to PUR. The grafted graphene oxide reinforced the PUR significantly through hydrogen bonds on the filler-rubber interfaces. Additional strain energy was dissipated by destructing the hydrogen bond sacrificial unit during the strain process, thereby the strength and toughness were improved simultaneously.

2. Experiment

2.1. Materials. Polyurethane rubber (PUR, type of HA-5) was purchased from Shanxi Institute of Chemistry Industry, China. Graphene oxide (GO, lamellar size of 10-50 μm, layers of 6~10) was purchased from SuZhou Tanfeng Co., Ltd., China. Polyethylene glycol (PEG, AR, number-average molecular weight of 600), 4-dimethylaminopyridine (DMAP, AR), N, N'-dicyclohexylcarbodiimide (DCC, AR), and dicumyl peroxide (DCP, AR) were purchased from Sigma Aldrich Company, USA. All materials were used directly without further treatment.

2.2. Sample Preparation

2.2.1. Preparation of Grafted Graphene Oxide with Polyethylene Glycol. 600 mg GO and 350 ml toluene were added to a 500 ml single-neck flask at room temperature and dispersed by ultrasound for 30 minutes. Then 2.0 g PEG, 0.58 g DMAP, and 1.19 g DCC were added to the flask successively and dispersed by ultrasound for 30 minutes; thereafter, the content was stirred by magnetic force for 24 h at temperature 75°C. The reaction product was filtered by polytetrafluoroethylene filter paper with 0.2 μm aperture. Filter cake was washed with 50 ml of toluene and 700 ml of deionized water in turn and then was dried in vacuum oven at 60°C. The product was denoted as MGO. The preparation process was depictured in Figure 1.

2.2.2. Preparation of PUR/MGO. A mill (type of XK-150, Zhanjiang Machinery Factory, China) was used to mix the raw materials. The roller gap of mill was adjusted to about 0.1 mm, then PUR, GO (or MGO), and DCP were added in turn. After each addition, the PUR compounds were side-cut both sides in turn 5 times and then triangle-packed 5 times and thin-passing 5 times; finally, the rubber compounds were rolled into 2 mm sheet. After being parked for 24 h, the sheet was vulcanized on a press (type of KSH-R100, Dongguan Kesheng Industrial Co., Ltd., China) with 16 MPa for t_{90}+2 min at 175°C. The mass ratio of PUR: DCP was 100: 2. The amount of GO or MGO was variable. For example, if the amount of MGO was 0.5 phr, the sample was marked as PUR/MGO-0.5%.

2.3. Characterizations. The chemical structure of samples was characterized by an 8400S FTIR spectrometer (Shimadzu, Japan). The scanning range was 4000~400 cm^{-1}, the scanning time was 32, and the sample was produced by pressing potassium bromide troche.

Raman spectrum was determined by a LabRAM Aramis Raman microscope (HORIBA Jobin Yvon, France). The excitation source was He-Ne laser and the excitation wavelength was 532.0 nm.

The crystalline structure was analyzed using a D8 X-ray diffractometer (Bruker, Germany). The radiographic source was Cu-Kα, the accelerated voltage was 40 kV, the emission current was 40 mA, the scanning speed was 0.1 s/step, and the scanning range was 2θ=5~60°.

The thermal stability was characterized by a 209 F3 thermogravimetric analyzer (Netzsch, Germany). The examination range was 50~900°C for GO and MGO fillers, and the examination range was 50~800°C for PUR rubber. The heating rate was 30 K/min and the nitrogen stream was 20 ml/min.

The GO/PEG samples for FTIR, Raman spectra, X-ray diffraction test (XRD), and thermogravimetric test (TGA) were purified by reflux condensation with toluene for 2 h, then washed with 50 ml toluene and dried.

The dynamic mechanical properties were performed on a 214E dynamic mechanical analyzer (Netzsch, Germany) at stretching mode with a heating rate of 3 K/min from -80~60°C. The exciting frequency was 5 Hz and the amplitude was 60 μm.

The tensile properties were measured with a 2080 tensile testing machine (UC, Taiwan) according to the GB/T 528-2009, the thickness of specimens was 1.0 mm, the tensile speed of cyclic tension-recovery test was 50 mm/min, and the tensile speed of tensile strength test was 200 mm/min. The sample shape was a dumbbell-shaped strip.

The structure and morphology were recorded by a TM3030 scanning electron microscopy (Hitachi, Japan). The acceleration voltage was 15 kV and the samples were first sputtered with platinum film before measurement. The investigated surface was the tensile fracture surface.

3. Results and Discussion

3.1. Interface Structures of GO/PEG. The FTIR analyses were used to detect the molecular bonds' details of the GO, MGO, and PEG. MGO, GO, and PEG were analyzed with FTIR and the obtained spectra were shown in Figures 2(a) and 2(b). Compared with GO, the peak intensity of MGO at 3440 cm^{-1}, 2921 cm^{-1} and 1105 cm^{-1} was bigger. These three peaks correspond to the stretching vibration of the O-H bond, C-H bond, and C-O-C bond, respectively [22]. At 1257 cm^{-1} and 831 cm^{-1}, two new peaks appeared in MGO, which resulted from the stretching vibration of the C-O bond and the out-of-plane bending of O-H bond. All of these changes came from the grafting of PEG, which indicated that the PEG interacted with GO and successfully grafted on the surface of GO.

Raman spectroscopy can effectively characterize the crystal structure and charge transfer of GO. The Raman spectra of GO and MGO were shown in Figure 2(c). It can be seen from the figure that GO had two distinct characteristic peaks at 1580 cm^{-1} and 1342 cm^{-1}, which correspond to G-band and D-band of GO, respectively [23]. MGO also exhibited the G-band and D-band peaks, but the peak position of these two peaks shifted to 1589 cm^{-1} and 1334 cm^{-1}, respectively. This is because the interaction between PEG and GO leads to electron transfer [24]. In addition, the D-band is related to the vibration of sp^3 hybridized carbon and defects on the edges of GO formed during the oxidation. The G-band is caused by the vibration of sp^2 hybridized carbon in the graphite lattice. The intensity ratio of D-band and G-band (I_D/I_G) is commonly used to characterize the defects of graphene and monitor the functionalization of graphene [23]. The larger the I_D/I_G is, the more the C atomic lattice surface's defects exist. The smaller the I_D/I_G is, the less the C atomic lattice surface's defects exist. The I_D/I_G of GO was 0.23, while that of MGO was 0.83, which was significantly higher than that of GO. This is because PEG was randomly grafted on the GO surface by covalent bonds, resulting in the increase of the surface defects.

Figure 2(d) showed the TGA analysis curves of GO and MGO. The weight loss rate of GO at 200~900°C was only 2.01%, which was caused by the decomposition of oxygen-containing functional groups in the sample, while the weight loss rate of MGO at 50~200°C was 12.5%, which was caused by the loss of adsorbed water in the sample. The weight loss rate at 200~900°C was 38.9%, which was mainly due to the ablation of polyethylene glycol molecules grafted on the surface of the sample. Secondly, it also includes the decomposition of oxygen-containing functional groups on the surface of the sample. Therefore, the graft ratio of polyethylene glycol on the surface of GO was about 37%.

XRD can characterize the crystalline structure before and after GO modification. The XRD diagrams of GO and MGO were shown in Figure 2(e). A narrow and strong diffraction peak appeared at 26.4° in the diagram of GO, corresponding to the interlayer spacing of 0.337 nm. In addition, two weaker diffraction peaks appeared at 44.6° and 54.6°, which were the typical peaks of the multilayer grapheme [25]. Compared with GO, MGO also showed diffraction peaks at these three places, which indicated that the addition of PEG on the surface of GO did not affect the crystalline structure of GO, nor did it affect the interlayer spacing of GO sheets. What is more, MGO had a diffuse peak near 22°, which could ascribe to the addition of PEG. PEG was an amorphous substance, which was grafted to the surface of GO by the covalent bond and led to the appearance of diffuse peak [26].

3.2. Thermal Stability of PUR/MGO Composites. The thermogravimetric analyses of PUR, PUR/GO, and PUR/MGO vulcanizates were shown in Figure 3 and Table 1. Compared with the pure PUR vulcanizate, the initial decomposition temperature (T_i), maximum decomposition temperature (T_{max}), and termination decomposition temperature (T_t) of the vulcanizate added with 0.5% GO were increased by 1.9°C, 16.8°C, and 17.8°C, respectively. Meanwhile, the T_i, T_{max}, and T_t of the vulcanizate added with 0.5% MGO were increased by 2.7°C, 18.9°C, and 22.9°C, respectively. When the addition

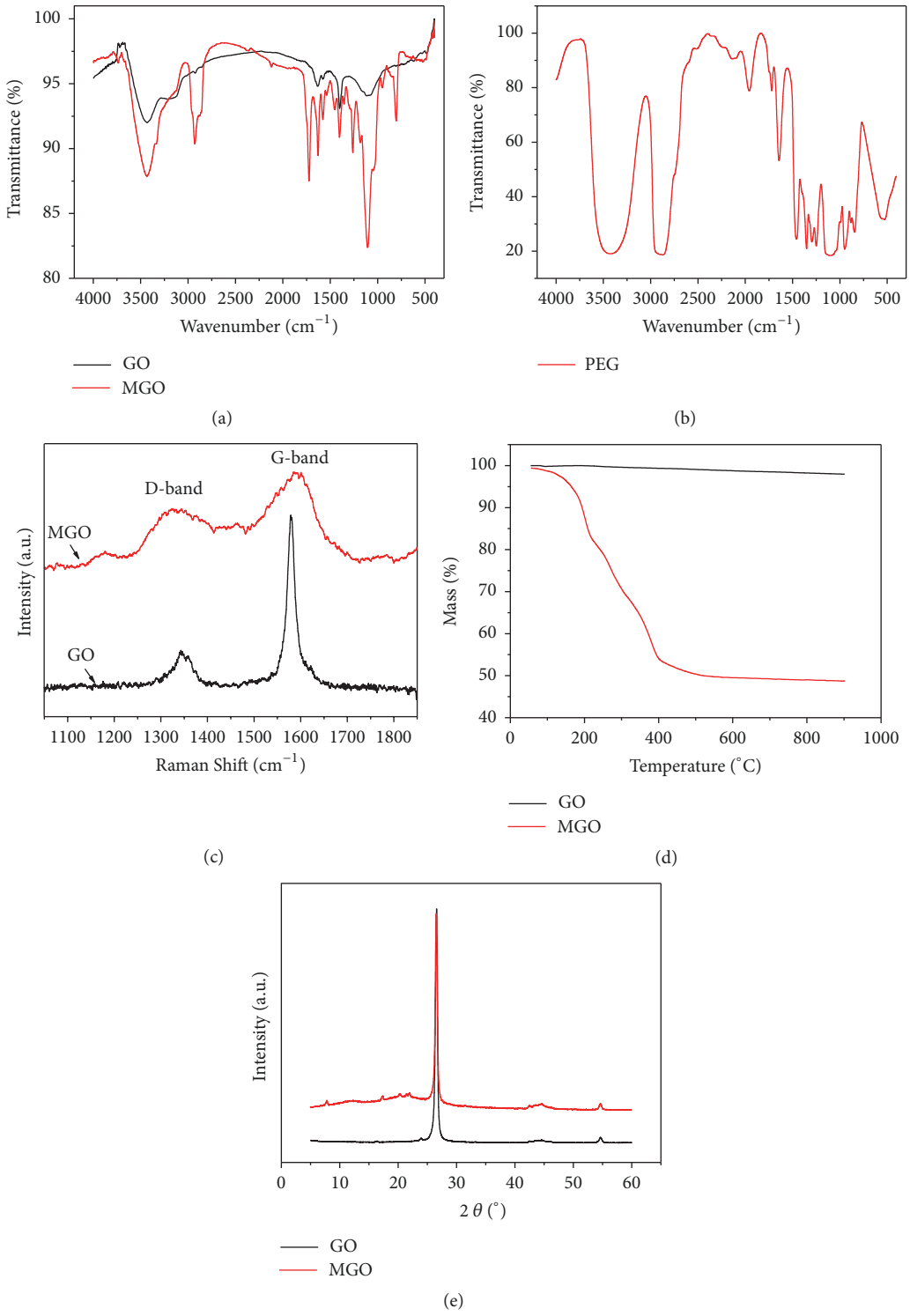

Figure 2: Structural characterizations of GO, MGO, and PEG. (a) FTIR characterization of GO and MGO; (b) FTIR characterization of PEG. (c) Raman spectra characterization of GO and MGO; (d) TGA characterization of GO and MGO; (e) XRD characterization of GO and MGO.

of GO or MGO were increased to 1%, the T_i, T_{max}, and T_t of the vulcanizates were increased again. This indicated that the addition of GO or MGO was helpful for improving the thermal stability of the vulcanizates. This improvement phenomenon was the same as the addition of a filler such as carbon black to the rubber matrix to improve the thermal stability of the vulcanizate [27]. In addition, the thermal stability of MGO-added compounds was better than that of GO-added compounds at the same dosage, because MGO was dispersed better in the rubber matrix after the graft

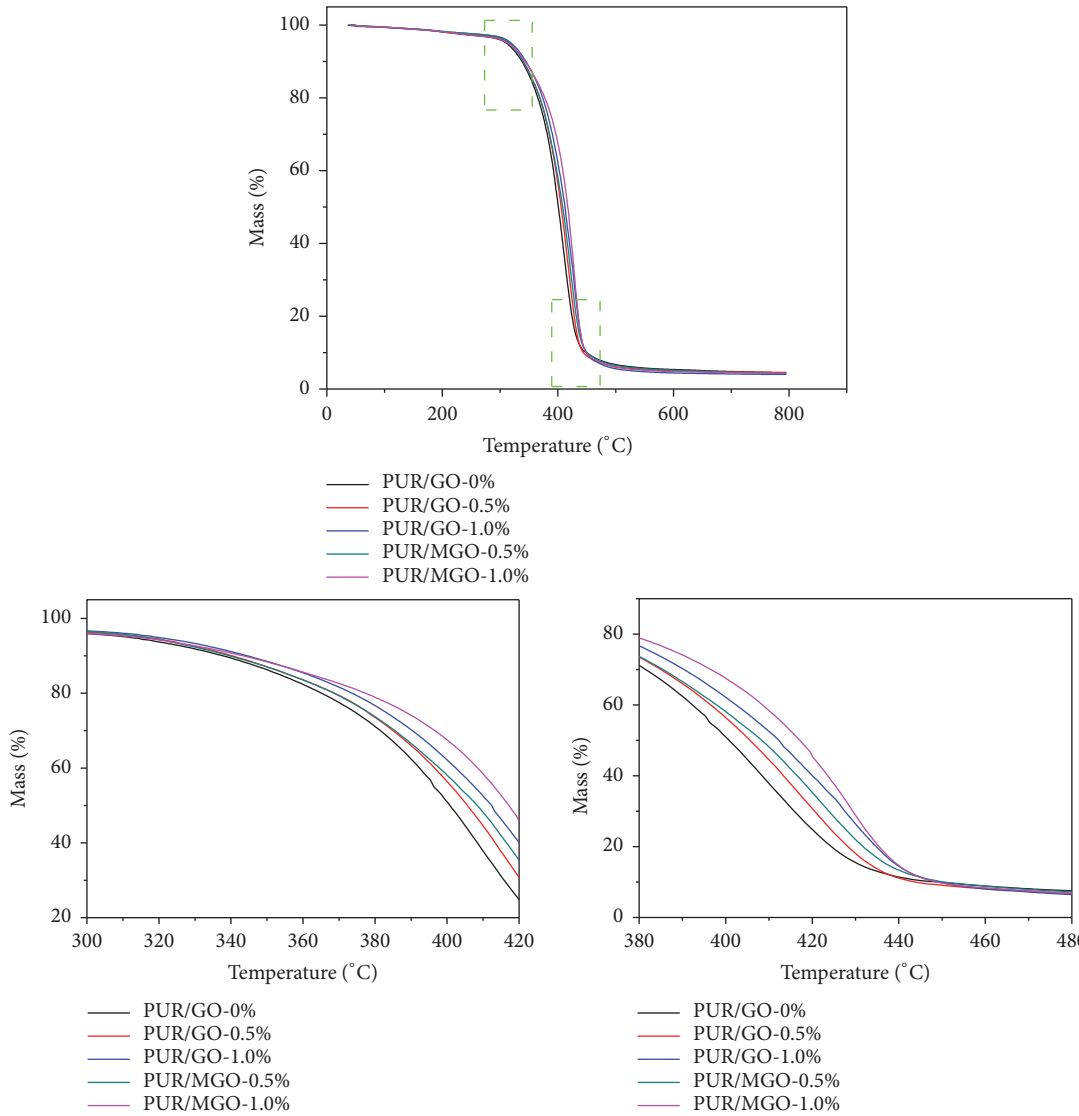

Figure 3: Thermogravimetric analyses of PUR, PUR/GO, and PUR/MGO composites.

Table 1: The key data of thermogravimetric analyses of PUR, PUR/GO, and PUR/MGO composites.

Sample	T_i(°C)	T_{max} (°C)	T_t(°C)
PUR/GO-0%	388.8	395.7	404.4
PUR/GO-0.5%	390.7	412.5	422.2
PUR/GO-1.0%	402.4	418.9	439.5
PUR/MGO-0.5%	391.5	414.6	427.3
PUR/MGO-1.0%	411.0	420.3	442.8

modification and formed stronger interaction with rubber molecular chains through molecular hydrogen bond [28]. What is more, after adding GO or MGO, the increasing range of the T_{max} and T_t of the vulcanizate was larger than that of the T_i. This is because GO or MGO is a lamellar structure, which would form a physical fire barrier layer in the rubber matrix after high-temperature combustion. The escape of decomposition products was slowed down and the further degradation was delayed because of the existence of this fire barrier [29].

3.3. Dynamic Mechanical Property of PUR/MGO Composites. The dynamic mechanical properties of PUR, PUR/GO, and PUR/MGO vulcanizates were shown in Figure 4. As can be seen from Figure 4(a), compared with the pure PUR vulcanizate, the initial storage modulus of the vulcanizate with GO or MGO was significantly increased. This is because the rigidity of the filler phase is much larger than that of the rubber phase, and the addition of a rigid filler phase to the flexible rubber phase produces a significant reinforcing effect

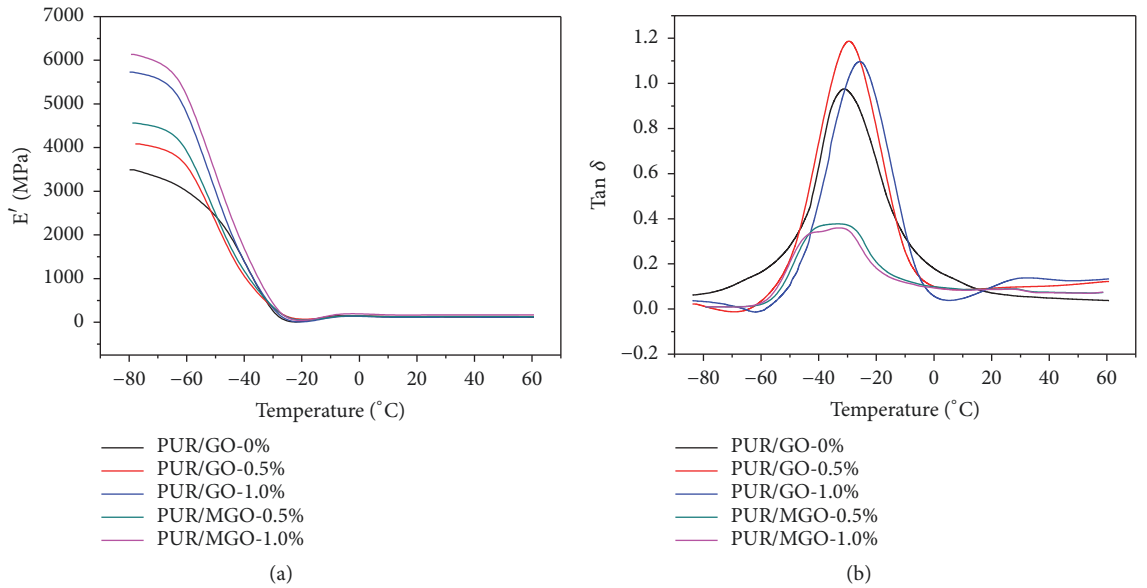

Figure 4: Dynamic mechanical properties of PUR, PUR/GO, and PUR/MGO composites.

[28]. This effect caused the initial storage modulus of vulcanizate to continue to increase when the filler phase content was increased from 0.5% to 1.0%. In addition, the storage modulus of PUR/MGO was larger than that of PUR/GO with the same filler content. This is due to the stronger interaction between MGO and PUR molecular chains [28].

The glass transition temperature (T_g) of elastomer can generally be obtained from the peak of the tan δ-temperature curve. It can be seen from Figure 4(b) that the T_g of the pure PUR vulcanizate was -30.8°C, and after adding 0.5% and 1.0% of GO, the T_g rose to -29.2°C and -25.5°C, respectively. It was shown that the addition of GO caused the T_g of vulcanizate to shift to higher temperature. This indicated that the low temperature resistance of vulcanizate decreased when GO was added. This is because the glass transition temperature is the reflection of the transition of the chain segments and the molecular chains motion form, and it is the lowest temperature for the molecular chain segments to have the motion ability in polymer. GO had a strong interaction with the rubber molecular chains, limiting the ability of the molecular chain to move, resulting in the increase of T_g. After the addition of MGO, the peak shape of the vulcanizate near the glass transition temperature had changed significantly, from the original high and sharp peak shape to a low and wide peak shape. In general, crystalline polymers exhibit a wide temperature range during the melting process. This temperature range is called the melting range, which is related to the melting of crystals with different crystallinity at different temperatures. Similarly, PUR/MGO composites also exhibit a wide temperature range during the glass transition process. This temperature range can be called the glass transition range of the polymer, which should be related to the multiple motion mechanisms of the molecular chains in PUR/MGO composites. During the dynamic strain process of PUR/MGO, besides the movement of microrubber molecular chain segments, the destruction and recombination of hydrogen bonds between rubber molecular chains and MGO surfaces were also included. This destruction and recombination of hydrogen bonds will dissipate a portion of the energy, resulting in the change of the tan δ peak shape. In addition, the glass transition range of PUR/MGO-0.5% was -30.4~-40.3°C, and the glass transition range of PUR/MGO-1.0% was -31.6~-42.7°C. Unlike the movement rule of the glass transition temperature of the vulcanizate with GO, the glass transition temperature of the vulcanizate was shifted to lower temperature, and the low temperature resistance of the material was increased after the addition of MGO. This is because the movement of hydrogen bonds is a kind of secondary transformation and can take place at lower temperature. This also explains why the glass transition temperature of PUR/MGO-1.0% was lower than that of PUR/MGO-0.5% because more hydrogen bonds were formed.

3.4. Tensile Properties of PUR/MGO Composites. The introduction of sacrificial hydrogen bonds in PUR matrix could improve the toughness of the material, which could be proved by the cyclic tension-recovery curve of vulcanizate. When the PUR, PUR/MGO-0.5%, and PUR/MGO-1.0% samples were respectively stretched to a preset strain of 100%, the values of the hysteresis loops were 33.03, 38.66, and 42.99, respectively (Figure 5(a)). It can be seen that the obvious hysteresis loss occurred after adding MGO, and the value of hysteresis loss was increased with the increase of MGO content. This is because the hydrogen bonds will be produced when MGO was added to the PUR matrix, and the hydrogen bonds in the PUR matrix were destroyed during the stretching process and a large amount of energy was dissipated, which led to the increase of hysteresis loss.

However, hydrogen bond is reversible, and it can be regenerated during the storage or heat treatment of material

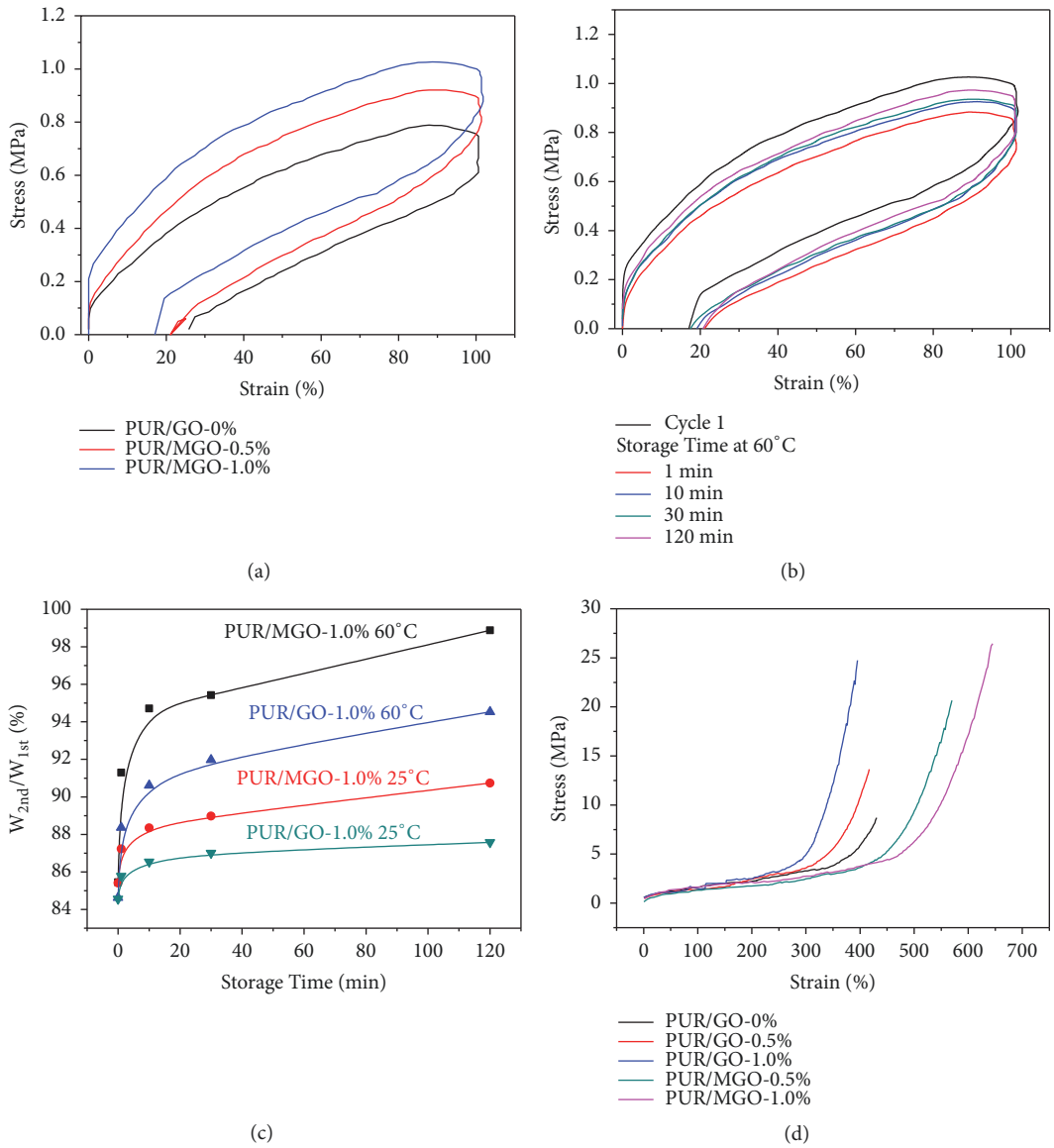

Figure 5: Tensile properties of PUR, PUR/GO, and PUR/MGO composites.

to achieve dynamic reversibility. In general, the recovery of hydrogen bond is dependent on the time and temperature. Taking PUR/MGO-1.0% as an example, the cyclic tension-recovery curves of PUR/MGO-1.0% vulcanizate with different recovery time at 60°C were discussed (Figure 5(b)). It can be found that hydrogen bonds can spontaneously recover during high-temperature storage, which leaded to a gradual increase of hysteresis loss.

The hysteresis loss recovery of PUR/GO-1.0% and PUR/MGO-1.0% under different conditions was quantitatively compared in Figure 5(c). W_{1st} was the initial tension-recovery hysteresis loss of the sample, and the W_{2nd} was the tension-recovery hysteresis loss of the samples after it had recovered for a certain time at a certain temperature. Firstly, with the prolongation of storage time, the hysteresis loss of PUR/GO-1.0% gradually recovered, which was related to the recrimping, reentanglement of microrubber molecular chains and the interaction recovery of filler-rubber molecular chains. Under the same storage time, the recovery rate of hysteresis loss of PUR/MGO-1.0% was higher than that of PUR/GO-1.0%. This was because, for PUR/MGO-1.0% sample, besides the recrimping, reentanglement of microrubber molecular chains and the interaction recovery of filler-rubber molecular chains, the regeneration of hydrogen bonds also led to an increase of recovery rate. Secondly, the recovery rate was increased with the increase of the storage temperature. The recovery rate of PUR/GO-1.0% was 87.58% after storage at 25°C for 120 min, and the recovery rate was increased to 94.53% after storage at 60°C for 120 min. The recovery rate of PUR/MGO-1.0% was 90.74% after storage at 25°C for 120 min, and the recovery rate was increased to 98.88% after storage at 60°C for 120 min. In addition, under the same storage temperature, the recovery rate of the samples with MGO was higher than that of samples with GO. This is not

only related to the recrimping, reentanglement of microrubber molecular chains and the recovery of the interaction between fillers and rubber molecular chains, but also to the faster spontaneous recovery of dissociated hydrogen bonds at higher temperature.

The stress-strain curves of PUR, PUR/GO, and PUR/MGO vulcanizates were shown in Figure 5(d). The tensile strength and elongation at break of pure PUR vulcanizate were 8.65 MPa and 431%. After adding 0.5% GO, the tensile strength of the vulcanizate was increased to 13.64 MPa and the increase rate was 57.7%, but the elongation at break was decreased to 417%, and the decrease rate was 3.2%. When the amount of GO was increased by 1%, the tensile strength of the vulcanizate continued to rise to 24.75 MPa, the rate of increase was 186.1%, the elongation at break was decreased to 395%, and the decrease rate was 8.4%. It was shown that the tensile strength of vulcanizate was improved with the increase of GO content, but the elongation at break was decreased. That is, the strength of vulcanizate was increased and the toughness was decreased when GO was added. However, after adding 0.5% MGO, the tensile strength of the vulcanizate was increased to 20.65 MPa, the increase rate was 138.7%, the elongation at break was increased to 570% at the same time, and the increase rate was 32.2%. When the amount of MGO was increased by 1%, the tensile strength of the vulcanizate continued to rise to 26.44 MPa, the increase rate was 205.7%, the elongation at break continued to rise to 645%, and the increase rate was 49.6%. It can be seen that the addition of MGO is helpful for improving the strength and toughness of vulcanizate simultaneously.

3.5. SEM Analyses of PUR/MGO Composites. SEM can be used to analyze the dispersion of fillers in rubber matrix and the interactions between the filler and rubber matrix. The tensile fracture surface of PUR, PUR/GO, and PUR/MGO vulcanizates were shown in Figure 6. As can be seen from the figures, the pure PUR vulcanizate had a relatively simple cross-section structure and the fracture surfaces were smooth in each fault (Figure 6(a)). After adding 0.5% GO or MGO, the fracture surfaces of the vulcanizates were rough, and the height difference between the cross-section layers was reduced. Moreover, the cross-section layers were parallel-peeled (Figures 6(b) and 6(c)). This indicated that there should be a kind of force perpendicular to the direction of tensile stress during the fracture of vulcanizate. This force should originate from the sheet exfoliation of graphene oxide lamellae from rubber matrix by the tensile force (as shown in the red circle in Figure 6(c)). When the amount of GO or MGO was added to 1%, the sense of layering of the cross-section tented to be more obvious (Figures 6(d) and 6(e)), because the filler and rubber matrix produced more sheet exfoliation. Comparing PUR/GO and PUR/MGO with 1% fillers (comparing Figure 6(d) with Figure 6(e)), it can be found that the sense of layering of the cross-section of the PUR/MGO was stronger than that of PUR/GO and the section of the PUR/MGO vulcanizate was rich and scattered. The reason was that the compatibility between the rubber matrix and GO was improved when GO was modified with PEG, and the dispersibility of MGO in the rubber matrix was also improved. Therefore, the interaction points between the fillers and the rubber molecular chains were increased, and the interaction force was improved.

3.6. Mechanism on Strengthening and Toughening PUR/MGO Composites. The strengthening and toughening mechanism of PUR/MGO composites was shown in Figure 7. In PUR/MGO system, continuous hydrogen bonds were formed between the PUR molecular chains and the PEG molecular chains which was grafted on the surface of GO by covalent bonds ($\lambda=\lambda_0$). During the stretching process, the PUR molecular chains were firstly oriented along the stress direction ($\lambda=\lambda_1$). If the strain was increased continuously ($\lambda=\lambda_2$, λ_3), the hydrogen bonds between PUR and PEG would be gradually dissociated, and the hydrogen bond interactions would be destroyed gradually with the increase of strain. A large amount of strain energy was consumed and the hidden length hid between the PUR molecular chains and the PEG molecular chains was released during the strain process. Thus, the tensile strength and toughness of the rubber material could be improved simultaneously. In PUR/MGO system, the PUR molecular chains had been cross-linked because of the presence of DCP vulcanizing agent. If the vulcanizate was not broken at the macroscopic level during the strain process, it will show macrorecovery under the action of the DCP permanent cross-linking bonds when the stress was removed. Meanwhile, the PEG molecular chains and the PUR molecular chains were close to each other at the microscopic level, which made it possible to regenerate hydrogen bonds between the PEG molecular chains and the PUR molecular chains during the storage or heat treatment process, and thereby the reversible recovery of hydrogen bonds was realized ($\lambda=\lambda'_0$).

4. Conclusions

The hydrogen bond sacrificial units were introduced into the PUR-MGO system by grafting PEG onto the surface of GO. The FTIR analysis showed the PEG was successfully grafted onto the surface of GO. The TGA analysis indicated the grafting rate was about 37%. The XRD analysis determined the addition of PEG did not affect the crystalline structure of GO. The hydrogen bond sacrificial units of PUR/MGO composites were destroyed and the hidden length was released during the stretching process, thereby the tensile strength and elongation at break were improved simultaneously. Compared with pure PUR vulcanizate, the tensile strength and elongation at break of PUR/MGO-1.0% were increased by 205.7% and 49.6%, respectively, while the tensile strength of PUR/GO-1.0% was increased by 186.1%, but the elongation at break was decreased by 8.4%. In addition, the addition of GO or MGO can improve the thermal stability of PUR, and the improvement of MGO was better. The T_g of PUR/GO-1.0% was increased by 5.3°C. However, the T_g of PUR/MGO-1.0% was shifted to lower temperature. What is interesting was that a kind of glass transition range appeared due to the introducing of hydrogen bonds. What is more, increasing

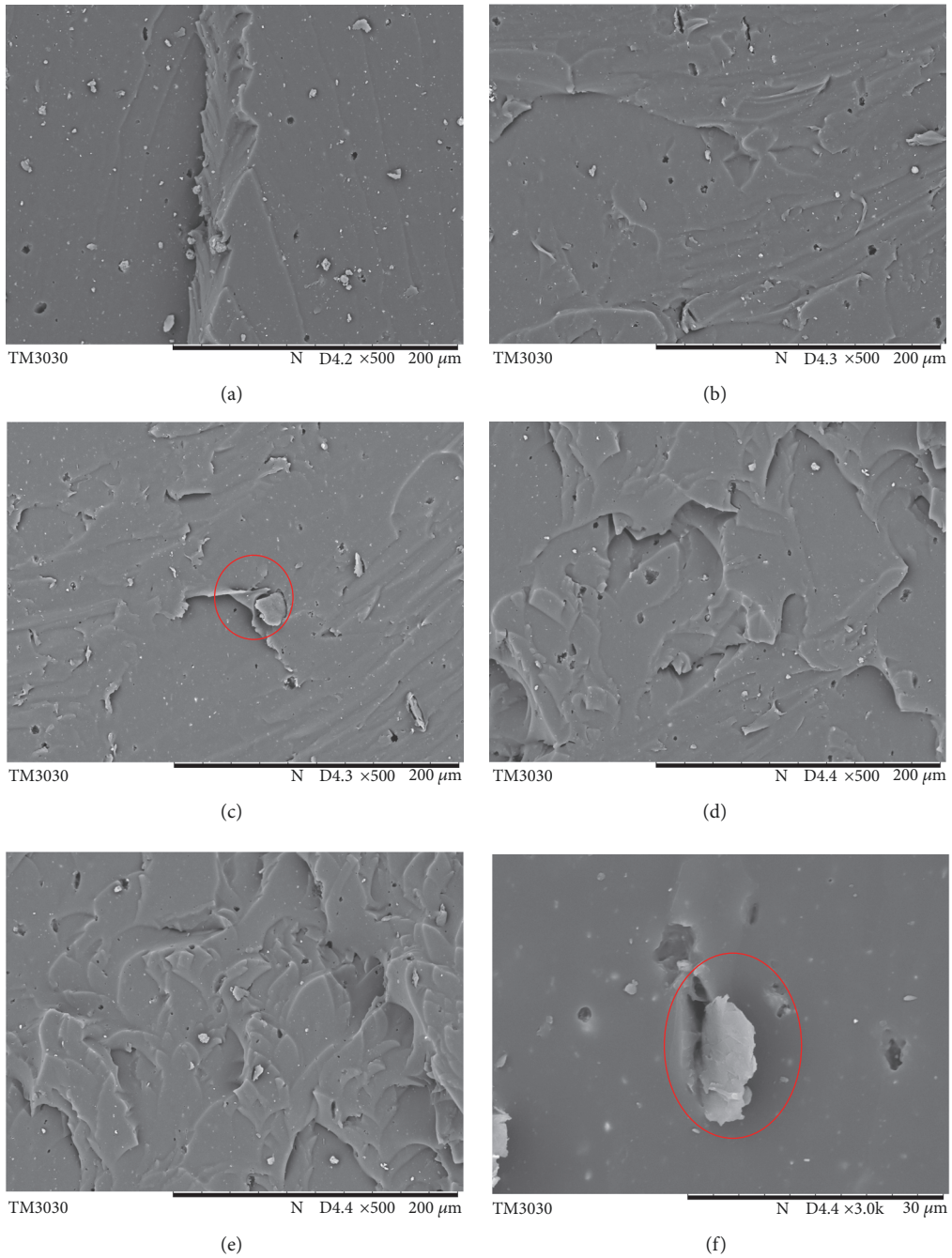

Figure 6: SEM analyses of PUR, PUR/GO, and PUR/MGO composites. (a) PUR/GO-0%; (b) PUR/GO-0.5%; (c) PUR/MGO-0.5%; (d) PUR/GO-1.0%; (e) PUR/MGO-1.0%; (f) PUR/MGO-1.0%.

the heat treatment temperature and prolonging the heat treatment time were helpful for the reversible recovery of hydrogen bonds.

Data Availability

The figure and table data used to support the findings of this study are included within the article.

Conflicts of Interest

The authors declare that they have no conflicts of interest.

Authors' Contributions

Li Wang and Wen Fu contributed equally to this paper.

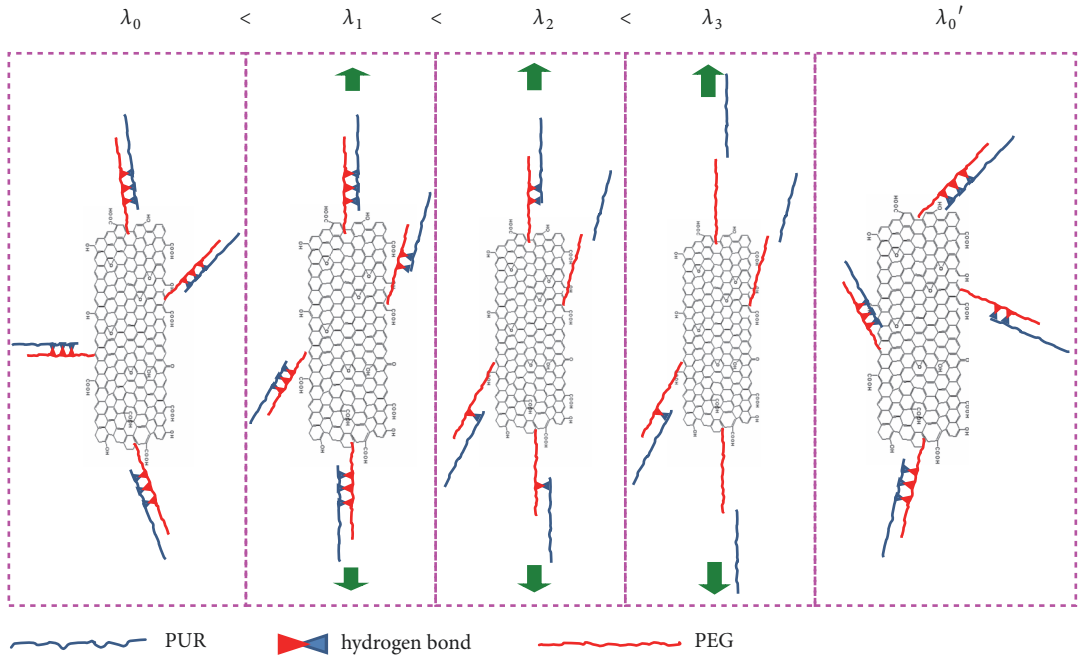

Figure 7: Strengthening and toughening mechanism of PUR/MGO composites.

Acknowledgments

This research was supported by Natural Science Foundation of Guangdong Province (2017A030310663, 2018A030307018, and 2018A0303070003), Distinguished Young Talents in Higher Education of Guangdong (2016KQNCX107), Guangdong Research Center for Unconventional Energy Engineering Technology (GF2018A005), and Maoming Science and Technology Project (Maokezi 2019 (33)).

References

[1] C. Lee, X. Wei, J. W. Kysar, and J. Hone, "Measurement of the elastic properties and intrinsic strength of monolayer graphene," *Science*, vol. 321, no. 5887, pp. 385–388, 2008.

[2] V. D. Punetha, S. Rana, H. J. Yoo et al., "Functionalization of carbon nanomaterials for advanced polymer nanocomposites: A comparison study between CNT and graphene," *Progress in Polymer Science*, vol. 67, pp. 1–47, 2017.

[3] S. He, N. D. Petkovich, K. Liu, Y. Qian, C. W. Macosko, and A. Stein, "Unsaturated polyester resin toughening with very low loadings of GO derivatives," *Polymer Journal*, vol. 110, pp. 149–157, 2017.

[4] M. Suominen, P. Damlin, S. Granroth, and C. Kvarnström, "Improved long term cycling of polyazulene/reduced graphene oxide composites fabricated in a choline based ionic liquid," *Carbon*, vol. 128, pp. 205–214, 2018.

[5] J. Wang, H. Jia, Y. Tang et al., "Enhancements of the mechanical properties and thermal conductivity of carboxylated acrylonitrile butadiene rubber with the addition of graphene oxide," *Journal of Materials Science*, vol. 48, no. 4, pp. 1571–1577, 2013.

[6] C. Wu, X. Huang, G. Wang et al., "Hyperbranched-polymer functionalization of graphene sheets for enhanced mechanical and dielectric properties of polyurethane composites," *Journal of Materials Chemistry*, vol. 22, no. 14, pp. 7010–7019, 2012.

[7] X. She, C. He, Z. Peng, and L. Kong, "Molecular-level dispersion of graphene into epoxidized natural rubber: morphology, interfacial interaction and mechanical reinforcement," *Polymer Journal*, vol. 55, no. 26, pp. 6803–6810, 2014.

[8] S. Keten, Z. Xu, B. Ihle, and M. J. Buehler, "Nanoconfinement controls stiness, strength and mechanical toughness of beta-sheet crystals in silk," *Nature Materials*, vol. 9, no. 4, pp. 359–367, 2010.

[9] M. E. Launey, M. J. Buehler, and R. O. Ritchie, "On the mechanistic origins of toughness in bone," *Annual Review of Materials Research*, vol. 40, no. 1, pp. 25–53, 2010.

[10] A. Gautieri, M. J. Buehler, and A. Redaelli, "Deformation rate controls elasticity and unfolding pathway of single tropocollagen molecules," *Journal of the Mechanical Behavior of Biomedical Materials*, vol. 2, no. 2, pp. 130–137, 2009.

[11] M. Hayashi, S. Matsushima, A. Noro, and Y. Matsushita, "Mechanical property enhancement of ABA block copolymer-based elastomers by incorporating transient cross-links into soft middle block," *Macromolecules*, vol. 48, no. 2, pp. 421–431, 2015.

[12] B. J. Gold, C. H. Hövelmann, C. Weiss et al., "Sacrificial bonds enhance toughness of dual polybutadiene networks," *Polymer Journal*, vol. 87, pp. 123–128, 2016.

[13] M. C.R., L. M., J. Y.L., S. L., and R. K. R.T., "Adsorption behaviour of reduced graphene oxide towards cationic and anionic dyes: Co-action of electrostatic and $\pi - \pi$ interactions," *Materials Chemistry and Physics*, vol. 194, pp. 243–252, 2017.

[14] J. Yuan, H. Zhang, G. Hong et al., "Using metal–ligand interactions to access biomimetic supramolecular polymers with adaptive and superb mechanical properties," *Journal of Materials Chemistry B*, vol. 37, no. 1, pp. 4809–4818, 2013.

[15] L. Zhang, L. R. Kucera, S. Ummadisetty et al., "Supramolecular multiblock polystyrene–polyisobutylene copolymers via ionic interactions," *Macromolecules*, vol. 47, no. 13, pp. 4387–4396, 2014.

[16] Z. Tang, J. Huang, B. Guo, L. Zhang, and F. Liu, "Bioinspired engineering of sacrificial metal–ligand bonds into elastomers with supramechanical performance and adaptive recovery," *Macromolecules*, vol. 49, no. 5, pp. 1781–1789, 2016.

[17] J. Huang, L. Zhang, Z. Tang et al., "Bioinspired design of a robust elastomer with adaptive recovery via triazolinedione click chemistry," *Macromolecular Rapid Communications*, vol. 38, no. 7, pp. 1600678–1600684, 2017.

[18] S. Wu, M. Qiu, Z. Tang, J. Liu, and B. Guo, "Carbon nanodots as high-functionality cross-linkers for bioinspired engineering of multiple sacrificial units toward strong yet tough elastomers," *Macromolecules*, vol. 50, no. 8, pp. 3244–3253, 2017.

[19] Y. Y. Mao, S. P. Wen, Y. L. Chen et al., "High performance graphene oxide based rubber composites," *Scientific Reports*, vol. 3, no. 3, pp. 2508–2514, 2013.

[20] W. Wu, C. Wan, S. Wang, and Y. Zhang, "Physical properties and crystallization behavior of ethylene-vinyl acetate rubber/polyamide/graphene oxide thermoplastic elastomer nanocomposites," *RSC Advances*, vol. 3, no. 48, pp. 26166–26176, 2013.

[21] S. M. Liff, N. Kumar, and G. H. McKinley, "High-performance elastomeric nanocomposites via solvent-exchange processing," *Nature Materials*, vol. 6, no. 1, pp. 76–83, 2007.

[22] D. Luo, F. Wang, B. V. Vu et al., "Synthesis of graphene-based amphiphilic Janus nanosheets via manipulation of hydrogen bonding," *Carbon*, vol. 126, pp. 105–110, 2018.

[23] X. Liu, W. Kuang, and B. Guo, "Preparation of rubber/graphene oxide composites with in-situ interfacial design," *Polymer Journal*, vol. 56, pp. 553–562, 2015.

[24] H. Sun, G.-L. Xu, Y.-F. Xu et al., "A composite material of uniformly dispersed sulfur on reduced graphene oxide: aqueous one-pot synthesis, characterization and excellent performance as the cathode in rechargeable lithium-sulfur batteries," *Nano Research*, vol. 5, no. 10, pp. 726–738, 2012.

[25] J. Zhang, Y. Xu, L. Cui et al., "Mechanical properties of graphene films enchanced by homo-telechelic functionalized polymer fillers via π–π stacking interactions," *Composites Part A: Applied Science and Manufacturing*, vol. 71, pp. 1–8, 2015.

[26] L. Zhang, R. Jamal, Q. Zhao, M. Wang, and T. Abdiryim, "Preparation of PEDOT/GO, PEDOT/MnO_2, and PEDOT/GO/MnO_2 nanocomposites and their application in catalytic degradation of methylene blue," *Nanoscale Research Letters*, vol. 10, pp. 148–156, 2015.

[27] Z. X. Ooi, H. Ismail, and A. A. Bakar, "A comparative study of aging characteristics and thermal stability of oil palm ash, silica, and carbon black filled natural rubber vulcanizates," *Journal of Applied Polymer Science*, vol. 130, no. 6, pp. 4474–4481, 2013.

[28] H. Lian, S. Li, K. Liu, L. Xu, K. Wang, and W. Guo, "Study on modified graphene/butyl rubber nanocomposites. I. Preparation and characterization," *Polymer Engineering & Science*, vol. 51, no. 11, pp. 2254–2260, 2011.

[29] J. R. Potts, D. R. Dreyer, C. W. Bielawski, and R. S. Ruoff, "Graphene-based polymer nanocomposites," *Polymer Journal*, vol. 52, no. 1, pp. 5–25, 2011.